Inorg. Chem. **2007**, *46*, 4937–4943

Isolated Heterometallic Cr_7Ni Rings Grafted on Au(111) Surface

Valdis Corradini,*,† Roberto Biagi,† Umberto del Pennino,† Valentina De Renzi,† Alessandro Gambardella,† Marco Affronte,† Christopher A. Muryn,‡ Grigore A. Timco,‡ and Richard E. P. Winpenny*,‡

CNR-INFM-S3 National Research Centre and Dipartimanto di Fisica, Università di Modena e Reggio Emilia, Via G. Campi 213/A, 41100 Modena, Italy, and School of Chemistry, The University of Manchester, Oxford Road, Manchester, M13 9PL, U.K.

Received December 18, 2006

A study of the deposition of heterometallic antiferromagnetically coupled rings onto gold surfaces is reported. Two new $\{Cr_7Ni\}$ rings, $[NH_2{}^nPr_2][Cr_7NiF_8(3\text{-tpc})_{16}]$ (**1**) (where 3-tpc = 3-thiophenecarboxylate) and $[{}^n BuNH_2CH_2CH_2SH][Cr_7NiF_8(O_2C{}^tBu)_{16}]$ (**2**) have been made and structurally characterized. They have been deposited from the liquid phase on Au(111) and the adsorbed molecules compared by means of scanning tunneling microscopy (STM) and X-ray photoemission spectroscopy (XPS). In both cases a two-dimensional distribution of individually accessible $\{Cr_7Ni\}$ heterometallic rings on the gold surface has been obtained, exploiting the direct grafting of sulfur-functionalized clusters. There is a competition between the chemisorption of the $\{Cr_7Ni\}$ clusters and a thiolic self-assembled monolayer (SAM) formed by free ligands. In **2**, the presence of a single sulfur ligand should force the molecule to graft with the ring axis normal to the surface. The cluster stability in the STM images and the S-2p energy positions demonstrate, for both functionalizations, the strength of the grafting with the gold surface.

Introduction

If molecular nanomagnets are to be used as elementary units for high-density data storage[1,2] and information processing, it will be necessary to address individual molecules. Binding them onto suitable substrates becomes crucial, and therefore, design of appropriate derivatives and the implementation of procedures to attach polymetallic molecules to surfaces need to be examined. Different approaches have been developed in order to build up a self-assembled monolayer (SAMs) of dodecanuclear manganese cages, conventionally called $\{Mn_{12}\}$, on metallic surfaces. The most studied is the single-step deposition strategy, where suitably thiol-functionalized $\{Mn_{12}\}$ clusters are deposited directly on gold, exploiting the strong sulfur−gold bond.[3−5] Recently an indirect two-step deposition approach has been developed by Coronado et al., which is based on the exploitation of the electrostatic interaction between polycationic $\{Mn_{12}\}$ clusters and a gold surface previously functionalized with an anionic SAM.[6]

For the exploitation of molecular nanomagnets as possible building blocks for a solid-state quantum computer, it is necessary to identify those systems that are best suited for the "qubit" encoding and manipulation.[7−9] A simple example of a spin cluster is represented by a finite chain made of an odd number of $S = {}^1/_2$ spin centers with a dominant antiferromagnetic coupling between nearest neighbors. Otherwise, a chain with an even number of spins with a suitable

* To whom correspondence should be addressed. E-mail: valdis@unimo.it (V.C.), richard.winpenny@man.ac.uk (R.E.P.W).
† Università di Modena e Reggio Emilia.
‡ The University of Manchester.

(1) Joachim, C.; Gimzewski, J. K.; Aviram, A. *Nature* **2000**, *408*, 541.
(2) (a) Caneschi, A.; Gatteschi, D.; Sessoli, R.; Barra, A. L.; Brunel, L. C.; Guillot, M. *J. Am. Chem. Soc.* **1991**, *113*, 5873. (b) Sessoli, R.; Tsai, H. L.; Schake, A. R.; Wang, S. Y.; Vincent, J. B.; Folting, K.; Gatteschi, D.; Christou, G.; Hendrickson, D. N. *J. Am. Chem. Soc.* **1993**, *115*, 1804. (c) Wernsdorfer, W.; Aliaga-Alcalde, N.; Hendrickson, D. N.; Christou, G. *Nature* **2002**, *416*, 406.
(3) Cornia, A.; Fabretti, A. C.; Pacchioni, M.; Zobbi, L.; Bonacchi, D.; Caneschi, A.; Gatteschi, D.; Biagi, R.; Del Pennino, U.; De Renzi, V.; Gurevich, L.; Van der Zant, H. S. J. *Angew. Chem., Int. Ed.* **2003**, *42*, 1645.
(4) Cornia, A.; Fabretti, A. C.; Pacchioni, M.; Zobbi, L.; Bonacchi, D.; Caneschi, A.; Gatteschi, D.; Biagi, R.; del Pennino, U.; De Renzi, V.; Gurevich, L.; Van der Zant, H. S. J. *J. Magn. Magn. Mater.* **2004**, *e725*, 272−276.
(5) Nait Abdi, A.; Bucher, J. P.; Rabu, P.; Toulemonde, O.; Drillon, M.; Gerbier, P. *J. Appl. Phys.* **2004**, *95*, 7345.
(6) Coronado, E.; Forment Aliaga, A.; Romero, F. M.; Corradini, V.; Biagi, R.; De Renzi, V.; Gambardella, A.; del Pennino, U. *Inorg. Chem.* **2005**, *44*, 7693.
(7) Meier, F.; Levy, J.; Loss, D. *Phys. Rev. B* **2003**, *68*, 134417.
(8) Leuenberger, M. N.; Loss, D. *Nature* **2001**, *410*, 789.
(9) Meier, F.; Levy, J.; Loss, D. *Phys. Rev. Lett.* **2003**, *90*, 047901.

10.1021/ic0624266 CCC: $37.00
Published on Web 05/17/2007

substitution of one spin center can give a total spin $S = {}^1/_2$. We have recently described many such rings made by Cr^{III} ions.[10−15] The precursor of this family is a molecular ring containing eight Cr^{III} ions disposed in an octagonal geometry, with chemical formula $[Cr_8F_8(O_2C^tBu)_{16}]$.[10,11] The wheel is antiferromagnetically coupled leading to an $S = 0$ ground state. In order to get the desired $S = {}^1/_2$ ground state, we have replaced a single chromium center with a nickel ion.[11−15] The ground state $S = {}^1/_2$ doublet is energetically well-separated from the first excited multiplet: at zero magnetic field $\Delta_0/k_B = 13$ K.[13] For the exploitation of heterometallic rings as single spin cluster "qubits", we here report the design of appropriate $\{Cr_7Ni\}$ derivatives and procedures to graft them onto metallic surfaces. The two derivatives are modified in chemically different ways, either by modifying the ammonium group used to template the $\{Cr_7Ni\}$ ring or by replacing the pivalate ligands with functionalized carboxylates.The results show a two-dimensional distribution of individually accessible $\{Cr_7Ni\}$ rings on the gold surface, exploiting the direct grafting of sulfur-functionalized $\{Cr_7Ni\}$ clusters.

Results and Discussion

Synthetic, Structural, and Magnetic Studies. The beauty of the coordination chemistry of the $\{Cr_7Ni\}$ rings is the ease with which functional groups can be introduced, without markedly diminishing the yield of the reactions.[12,16] The general reaction is

$$7CrF_3{\cdot}4H_2O + NH_xR_{(3-x)} + {}^1/_5[2NiCO_3{\cdot}3Ni(OH)_2{\cdot}4H_2O] + \text{excess } R'CO_2H \rightarrow [NH_{x+1}R_{(3-x)}][Cr_7NiF_8(R'CO_2)_{16}]$$

Here we have varied the carboxylate to 3-thiophenecarboxylic acid, producing **1**, and separately varied the template to 2-(butylamino)ethanethiol, giving **2**; both rings are formed in greater than 60% yield. Thus, we can very easily produce new variants to study the factors involved in surface binding.

The crystal structures of both **1** and **2** show the formation of an octagon of metal centers, with each edge of the octagon bridged by a single fluoride and two 2.11-pivalates (Figure 1). The Cr···Cr distances along each edge in **1** fall in the range 3.294−3.473 Å while in **2** the range is narrower varying from 3.343 to 3.354 Å. The Cr−O and Cr−F bond lengths are unexceptional, given the problems with disorder in the structure, and not worth discussing. The template, ^{n}-$Pr_2NH_2^+$ in **1** and ^{n}BuNH$_2$CH$_2$CH$_2$SH in **2**, is held at the center of the octagon by N−H···F hydrogen bonds. There appears to be a difference between the two structures; in **1** the two shortest N···F distances are 3.11 Å, while in **2** there are two N···F contacts of 2.81 Å with two further contacts of 3.07 Å.

If we consider the dimensions of the cage compounds (which are important when we compare this with the images obtained by microscopy), we find that **1** has a maximum diameter of approximately 2.2 nm and a height of 1.5 nm. **2**, which contains pivalate rather than 3-thiophenecarboxylate, has a slightly smaller diameter of 1.8 nm and a height of 1.1 nm.

The magnetic properties of dried powders, characterized by means of ac susceptibility, are close to those previously reported for $\{Cr_7Ni\}$ derivatives. The spin Hamiltonian parameters are slightly changed but the ground state remains $S = {}^1/_2$ and there is still a gap between the ground state and the first excited state.

Scanning Tunneling Microscopy. A 2D distribution of $\{Cr_7Ni\}$ clusters on the Au(111) surface has been obtained from liquid-phase deposition. The two versions of the $\{Cr_7Ni\}$ ring investigated here both contain S-groups, which can be used to bind to a gold surface, but the number and orientation of these sulfurs is very different between the two molecules. In **2**, there is a single sulfur atom attached to the ring via the template at the center. This should force the molecule to bind while keeping the plane of the ring parallel to the surface and hence its easy magnetization axis normal to the surface. In **1**, there are sixteen 3-thiophenecarboxylates arranged in two groups: eight "equatorial" carboxylates which lie approximately in the plane of the $\{Cr_7Ni\}$ ring and eight "axial" carboxylates which are approximately perpendicular to the plane, alternately lying above and below the plane around the octagon. Although in this case we have less control of the orientation of the molecule with respect to the surface, we can expect a parallel orientation of the ring to be favored because if **1** binds with the ring plane parallel to the Au surface, four S atoms from the axial 3-tpc ligands can bond, while if **1** binds via the equatorial 3-tpc ligands, the attachment is likely to be through fewer sulfurs.

We have investigated the best conditions for the deposition of a submonolayer distribution of SMMs on gold, exploiting THF as a solvent. Different concentrations (from 1 to 9 mM) and different deposition times (from 10 s up to 20 h) have been examined. For immersion times below 30 s and concentrations lower than 0.5 mM, we do not observe any cluster adsorption. The highest cluster coverage, without formation of 3D aggregates, can be reached for concentrations ranging from 5 to 9 mM and does not significantly vary with immersion times in the range from 10 min up to 20 h. The deposition process was monitored by means of STM and XPS measurements. Typical imaging conditions are bias voltages of 2.0 V and a tunneling current of 30 pA,

(10) (a) Gerbeleu, V.; Struchkov, Y. T.; Timko, G. A.; Batsanov, A. S.; Indrichan K. M.; Popovich, G. A. *Dokl. Akad. Nauk SSSR* **1990**, *313*, 1459. (b) van Slageren, J.; Sessoli, R.; Gatteschi, D.; Smith, A. A.; Helliwell, M.; Winpenny, R. E. P.; Cornia, A.; Barra, A. L.; Jansen, A. G. M.; Rentschler, E.; Timco, G. A. *Chem.—Eur. J.* **2002**, *8*, 277.
(11) McInnes, E. J. L.; Piligkos, S.; Timco, G. A.; Winpenny, R. E. P. *Coord. Chem. Rev.* **2005**, *249*, 2577.
(12) Larsen, F. K.; McInnes, E. J. L.; Mkami, H. E.; Overgaard, J.; Piligkos, S.; Rajaraman, G.; Rentschler, E.; Smith, A. A.; Smith, G. M.; Boote, V.; Jennings, M.; Timco, G. A.; Winpenny, R. E. P. *Angew. Chem., Int. Ed.* **2003**, *42*, 101.
(13) Troiani, F.; Ghirri, A.; Affronte, M.; Carretta, S.; Santini, P.; Amoretti, G.; Piligkos, S.; Timco, G.; Winpenny, R. E. P. *Phys. Rev. Lett.* **2005**, *94*, 207208.
(14) Wernsdorfer, W.; Mailly, D.; Timco, G. A.; Winpenny, R. E. P. *Phys. Rev. B* **2005**, *72*, 060409.
(15) Affronte, M.; Troiani, F.; Ghirri, A.; Carretta, S.; Santini, P.; Corradini, V.; Schuecker, R.; Muryn, C.; Timco, G.; Winpenny, R. E. P. *Dalton Trans.* **2006**, 2810.
(16) Laye, R. H.; Larsen, F. K.; Overgaard, J.; Muryn, C. A.; McInnes, E. J. L.; Rentschler, E.; Sanchez, V.; Teat, S. J.; Güdel, H. U.; Waldmann, O.; Timco, G. A.; Winpenny, R. E. P. *Chem. Commun.* **2005**, 1125−1127

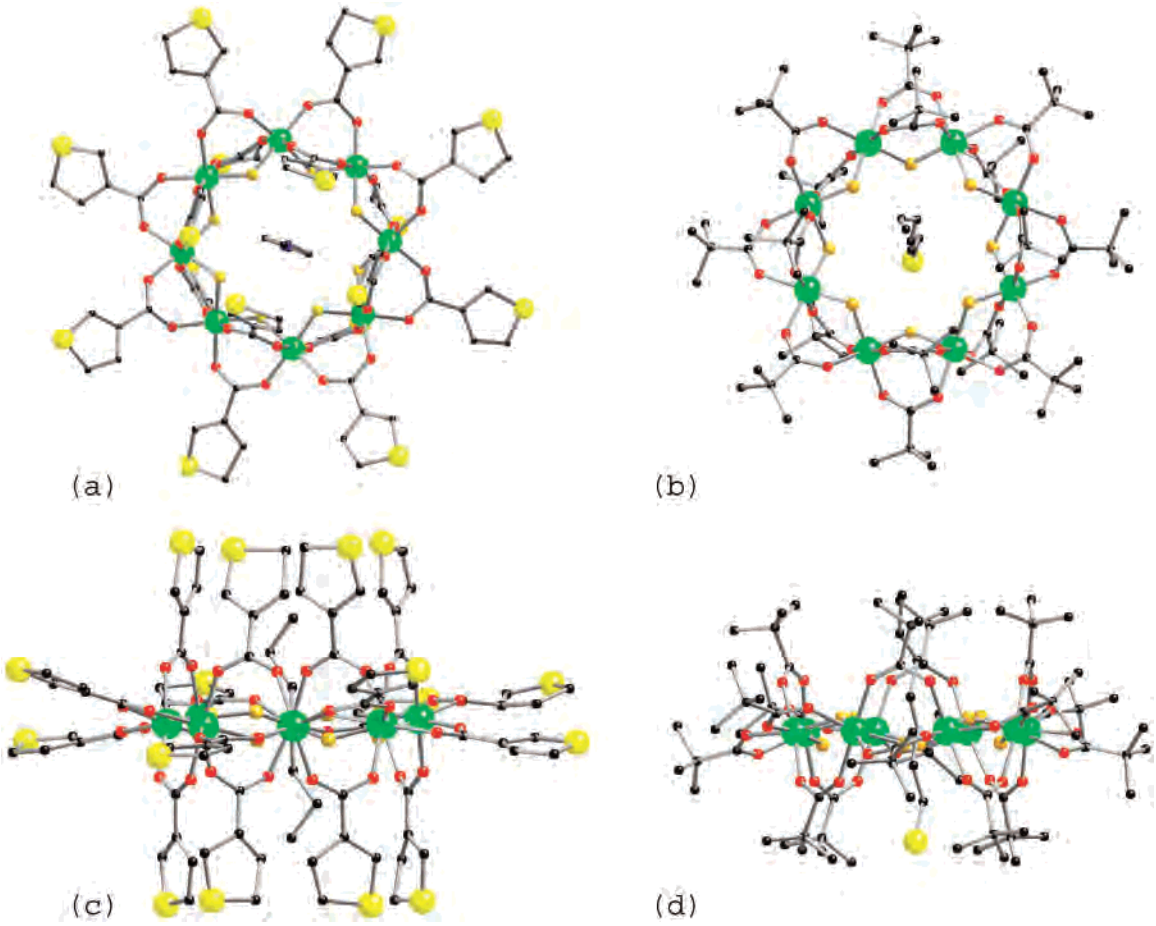

Figure 1. The structures of **1** and **2** in the crystal: (a) **1** viewed perpendicular to the Cr_7Ni plane; (b) **2** viewed perpendicular to the Cr_7Ni plane; (c) **1** viewed parallel to the Cr_7Ni plane; (d) **2** viewed parallel to the Cr_7Ni plane.

in order to minimize dragging and damaging of such soft organic materials with the scanning STM-tip. The best conditions were reached by immersing the Au(111) surface in a 5 mM solution of {Cr_7Ni} derivatives in THF for 10 min. After that, the substrate was rinsed in THF and immediately introduced into the UHV experimental chamber. Room-temperature STM images reported in Figure 2 reveal, for both systems, the presence of a quite homogeneous two-dimensional distribution of isolated {Cr_7Ni} clusters on the surface: there is no evidence of 3D aggregates (higher than 20 Å) and a very low number of 2D aggregates with diameters larger than 50 Å. The low level of noise and the stability of the clusters even at higher tunneling currents (up to 500 pA, they are not shifted by the scanning tip) confirms the strength of the molecular grafting with the Au surface, not only for **2**, which is strongly fixed by a single covalent S−Au bond, but also for **1**, where the grafting is secured by a few S atoms of the thiophene (TP) ligands interacting with the gold surface.

In both systems, the formation of vacancy islands (VI), 2.4 Å deep (corresponding to a monatomic Au terrace) and 50−100 Å wide,[17,18] indicates the presence of a first alkanethiol/TP SAM surrounding the clusters (the situation is sketched in Figure 3) as also confirmed by XPS results. The kinetics of formation of the VI is very different between the two samples. For **2**, we observe the VI formation after 10 min of immersion (see Figure 2 right panel), while for **1**, the VI become more evident only for a longer immersion time of 20 h (see Figure 3). In **2**, the formation of a complete alkanethiol SAM[17−19] indicates that the bond between the ring and the ammoniumthiol template breaks in solution. Although the 3-tpc should be more strongly attached to the cluster core through Cr−O bonds, the formation of the SAM[20,21] indicates that also in **1**, a fraction of TP ligands dissociate in solution. This kind of dissociation does not depend on the use of a polar solvent (THF) because VI formation has been observed also with a nonpolar solvent (toluene). The longer time required for the formation of a densely packed TP SAM with respect to the alkanethiol can be explained by a lower mobility of the adsorbed TP molecules bonded to gold.[20]

From the STM line-profiles, reported in Figures 2b and 3, a higher value is found for the diameter of **1** (4.0 ± 0.5 nm) than for **2** (3.5 ± 0.5 nm). This result is in agreement with the expected dimensions of the functionalized clusters (the ring diameter is 2.2 and 1.8 nm, respectively) convoluted

(17) Poirier, G. E. *Langmuir* **1997**, *13*, 2019.
(18) Yang, G.; Liu, G. *J. Phys. Chem. B* **2003**, *107*, 8746.
(19) Esplandiù, M. J.; Hagenstrom, H.; Kolb, D. M. *Langmuir* **2001**, *17*, 828.
(20) Noh, J.; Ito, E.; Nakajima, K.; Kim, J.; Lee, H.; Hara, M. *J. Phys. Chem. B* **2002**, *106*, 7139.
(21) Noh, J.; Ito, E.; Araki. T.; Hara, M. *Surf. Sci.* **2003**, *1116*, 532−535.

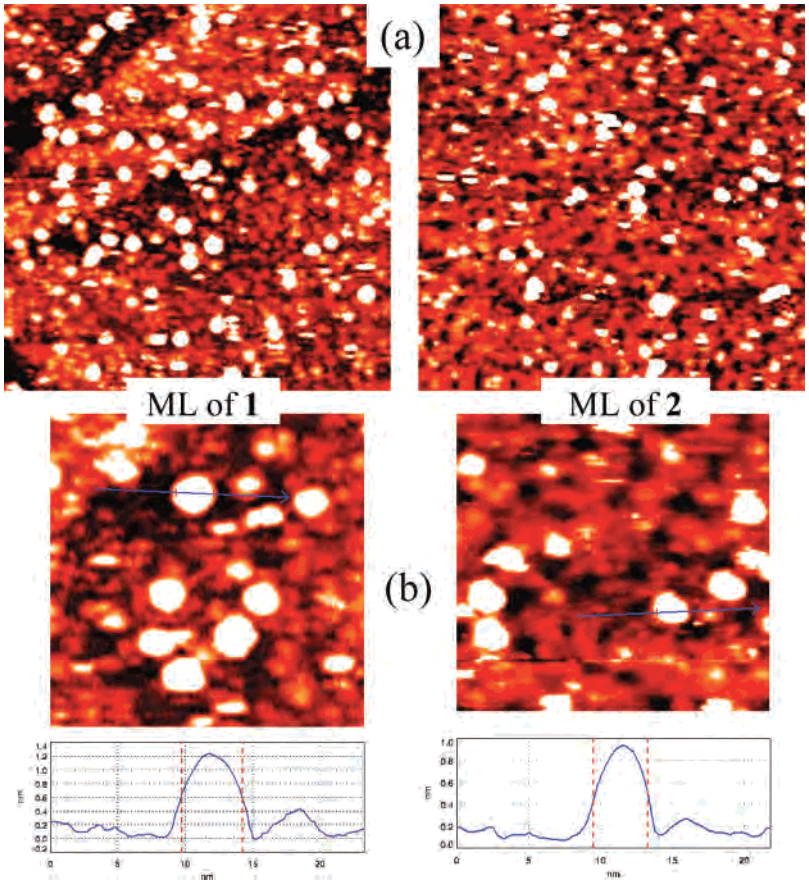

Figure 2. Constant-current (30 pA, 2 V) STM images of the Au(111) surface immersed for 10 min in a 5 mM solution of **1** (left panel) and **2** (right panel) derivatives in THF: (a) 100 × 100 nm^2 and (b) 35 × 35 nm^2 extended regions. The white entities represent the grafted clusters, and the black areas are the vacancy islands (VI). The STM height-profiles of the two Cr_7Ni derivatives are compared.

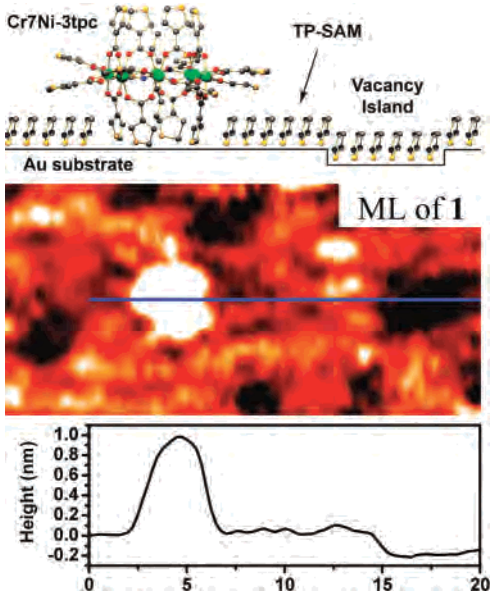

Figure 3. STM image (24 × 12 nm^2) of the Au(111) surface immersed for 20 h in a 5 mM solution of **1** (central panel) and height profile of a single cluster and of a VI (lower panel). The situation is sketched in the upper panel: each cluster is surrounded by a SAM formed by free ligands.

with the curvature radius of the tip, having assumed the ring is lying flat on the surface. The height derived from an STM profile depends on both sample topography and electronic contribution. However, assuming that the electronic contribution of the external organic region of the cluster, sampled by the STM tip, is similar to that of the SAM, the STM profile can be directly linked to the sample topography. The height of the clusters of **1** (1.0 ± 0.1 nm, see Figure 3) is larger than for **2** (0.8 ± 0.1 nm, see Figure 2b). In both cases the height is lower than that expected for the clusters (1.5 and 1.1 nm, respectively), confirming the presence of a first SAM of free alkanethiol\TP ligands (about 0.5−0.6 nm height), which surrounds the clusters (see upper panel of Figure 3).

From a statistical analysis of the STM images, we have derived a denser packing for the ML of **1**, with about 16−24% of the surface occupied by a 2D distribution of isolated clusters, while for **2** the coverage is only 5−8% of the total surface. The corresponding average area occupied by a single cluster is 20 ± 5 nm^2 for **1** and 40 ± 10 nm^2 for **2**. Although the isotropic shape of the functionalized clusters and the presence of a first SAM surrounding the clusters do not allow a clear identification of the ring axis orientation, the STM height profiles agree with a preferred "quasi-flat" orientation of the rings, with their axes preferentially lying in a cone normal to the surface. This is observed not only for **2**, where the presence of a single sulfur ligand should force the molecule to bind with its axis normal to the surface, but also for **1**. The predominant flat orientation of **1** on the surface may occur because it maximizes the number of S−Au interactions between the 3-tpc ligands and the gold surface.

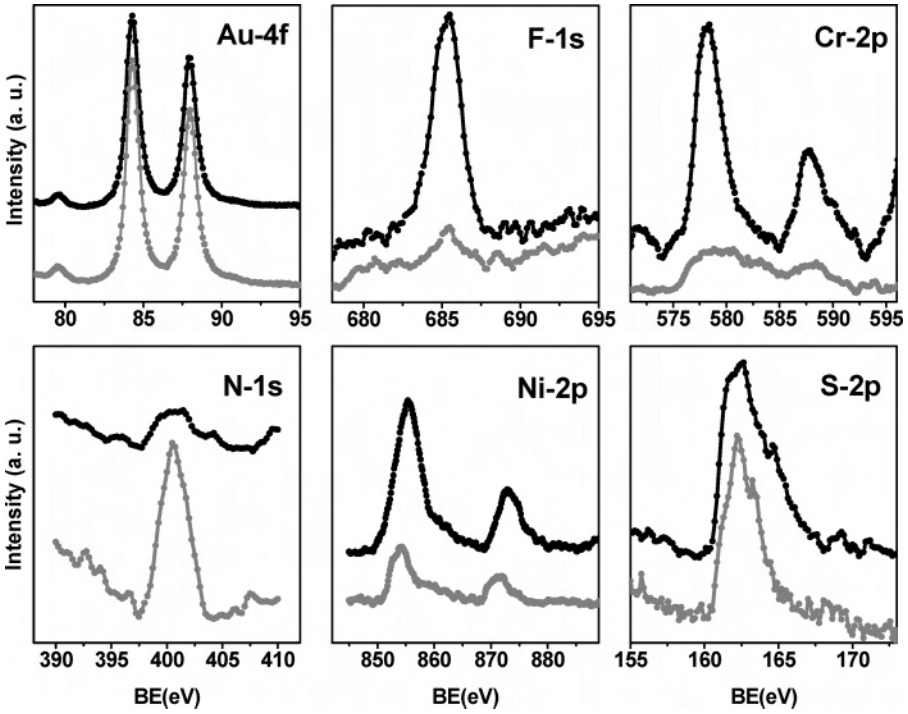

Figure 4. Core level XPS spectra for Au(111) surface immersed for 10 min in a 5 mM solution of **1** (upper spectra) and **2** (lower spectra) in THF. The background contribution has been subtracted.

Table 1. Coverages Derived from the Core Level Intensities of **1** and **2** Monolayers Compared with Values Derived from STM

	F-1s/Cr-2p	Cr-2p/Ni-2p	Au-4f/(S1 + S2)	SAM packing/Å^2/mol	Au-4f/Cr-2p	XPS coverage/%	STM coverage/%
monolayer of **1**	1.09 ± 0.05	6 ± 2	22 ± 2	20−26	150 ± 30	22−30	16−24
monolayer of **2**	1.13 ± 0.05	5 ± 2	27 ± 2	23−31	500 ± 100	6−9	5−8
expected value	1.14	7					

X-ray Photoelectron Spectroscopy (XPS). The STM results are confirmed by quantitative XPS investigations. In Figure 4, the core levels of the Au(111) surface immersed for 10 min in a 5 mM solution of **1** (upper spectra) and **2** (lower spectra) in THF are compared. All the core level intensities have been normalized taking into account the atomic sensitivity and the attenuation of the electronic signal. The Cr-2p, F-1s, and Ni-2p core levels line-shapes measured for the monolayer fit well with the corresponding data obtained for a multilayer deposited from the liquid phase (not reported here), indicating that the ring stoichiometry is preserved. For both systems, the ratios F-1s/Cr-2p and Cr-2p/Ni-2p are close to the expected ones and reproducible in all runs (see Table 1), confirming the ring stability.

At variance, the Cr/S ratio is 0.04 ± 0.01 instead of 7 in **2** and 0.16 instead of 0.44 ($^7/_{16}$) in **1**, suggesting a large excess of sulfur and indicating the presence of a sulfur-containing monolayer surrounding the clusters. The ratio between the S-2p and the Au-4f signals confirms, for both systems, the presence of a complete alkanethiol/TP SAM, in agreement with STM findings. Moreover, from the Au-4f/Cr-2p ratio (see Table 1) and taking into account the gold signal attenuation due to the SAM and the clusters, we can derive an average area occupied by each cluster of 15 ± 3 nm^2/molecule in **1** and of 36 ± 8 nm^2/molecule in **2**. The corresponding values of coverage are 22−30% (the calculated area for **1** is 3.8 nm^2) and 6−9% (the calculated area for **2** is 2.5 nm^2), respectively, in good agreement with the values derived from STM (see Table 1). On the other hand, the N-1s core levels (each cluster contains only one amine at the center of the ring) are much more intense for the monolayer of **2** than for **1**, indicating a significant presence of an amine group in the SAM **2**. For a deep investigation of the interface composition, we isolated the inequivalent contributions to the S-2p core level (Figure 5). The S-2p fitting procedure has been performed using spin−orbit split doublet components (Voigt functions) with the following parameters: spin−orbit splitting of 1.2 eV, branching ratio of 0.5, Lorentzian width of 574 meV, and Gaussian width of 600 meV for all components.

For the monolayer of **2**, three components are observed at 161.4 eV (S2 peak), 162.2 eV (S1), and 163.3 eV (S3). S1 and S3 can be easily assigned to the thiolate S atoms bonded with gold and to unbound S of the second layer thiols, respectively.[22,23] The S-2p component at about 161 eV is usually assigned to isolated atomic S deriving from C−S bonding cleavage.[24,25] On the other hand, Ishida et al. give a different assignment, suggesting the presence of a thiol bounded through sulfur, in an sp configuration.[23] In both

(22) Castner, D. G.; Hinds, K.; Grainger, D. W. *Langmuir* **1996**, *12*, 5083.
(23) (a) Ishida, T.; Choi, N.; Mizutani, W.; Tokumoto, H.; Kojima, I.; Azehara, H.; Hokari, H.; Akiba, U.; Fujihira, M. *Langmuir* **1999**, *15*, 6799. (b) Ishida, T.; Hara, M.; Kojima, I.; Tsuneda, S.; Nishida, N.; Sasabe, H.; Knoll, W. *Langmuir* **1998**, *14*, 2092.
(24) Vericat, C.; Vela, M. E.; Andreasen, G.; Salvarezza, R. C.; Vazquez, L.; Martín-Gago, J. A. *Langmuir* **2001**, *17*, 4919.
(25) Liu, G.; Rodriguez, J. A.; Dvorak, J.; Hrbek, J.; Jirsak, T. *Surf. Sci.* **2002**, *505*, 295.

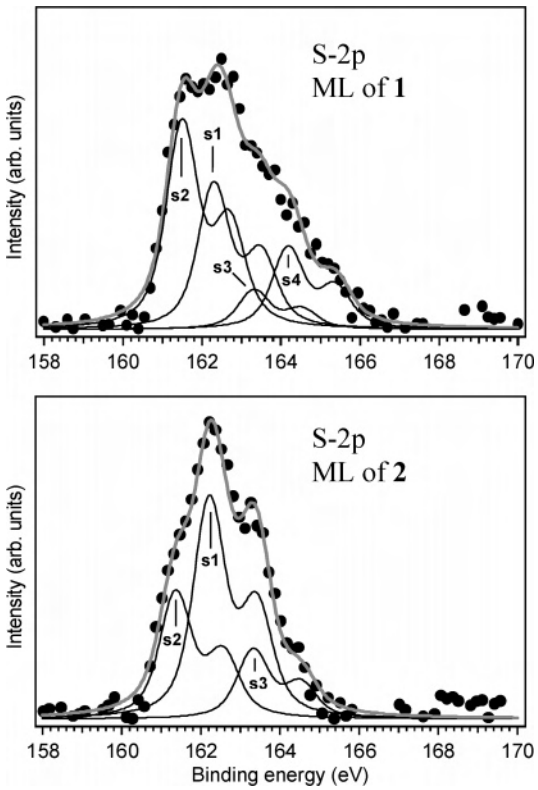

Figure 5. Comparison between S-2p core level fits for the ML of **1** (top panel) and **2** (bottom panel). The fitting parameters are reported in the text.

cases the S2 component is associated with a sulfur species bonded to gold. Thus, from the Au/(S1 + S2) ratio (reported in Table 1), we can derive a packing level for the first monolayer of 23−31 Å^2/S atom, comparable with previous STM studies on alkanethiol SAMs which indicate a packing level ranging from 22 to 34 Å^2/mol.[19] From the S3/(S1 + S2) ratio, we can derive that about 15% of the first SAM is covered by a second layer of unbound free alkanethiol ligands.

For the monolayer of **1**, four components are observed at 161.5 (S2), 162.3 (S1), 163.3 (S3), and 164.2 eV (S4). S1 and S2 have been observed in a few works on TP deposited from solution and assigned to S atoms of thiophene molecules chemisorbed on gold in two different adsorption geometries.[20,21] On the other hand, for the TP deposited from the gas phase in UHV, an S-2p peak at 163.9 eV has been reported, indicating a weak interaction with the gold surface.[25,26] A recent work of Sako et al.[26] suggests that the TP ring could break in solution due to the cleavage of one C−S bond. In this hypothesis, the grafting of the cluster would be assured by alkyl−thiolate chains instead of TP rings. Likewise the SAM would be formed by alkyl−thiolate chains identified by the characteristic S-2p peak at 162 eV. In both cases (TP molecules in different adsorption geometries or alkyl−thiolate deriving from broken TP rings), S1 and S2 are associated with two sulfur species bonded to gold. S3 and S4 are assigned to unbound TP molecules, which is in agreement with previous XPS investigations,[21,23a] they are attributed to the unbound sulfur originating from the physisorbed multilayer. Thus, from the Au/(S1 + S2) ratio (reported in Table 1), we can derive a packing level for the first monolayer of 20−26 Å^2/S atom, slightly higher than in the case of the monolayer of **2.** For each **1** cluster (7 Cr centers) there are probably 4 3-tpc ligands where the S is bonded with gold and 12 where the S is unbound (see Figure 3, top panel). Since the ratio S4/Cr = 1.5 ± 0.2 is reasonably in agreement with the expected value of 1.7 ($^{12}/_7$), we can suppose that S4 can be attributed to unbound S of 3-tpc ligands which are still bound to the cluster. S3 is then tentatively assigned to 3-tpc ligands which are separated from the core of the cluster but where the S− is not bound to Au. From the S3/(S1 + S2) ratio, we can derive that about 8% of the surface is covered by a second layer of unbound free TP ligand.

(26) Sako, E. O.; Kondoh, H.; Nakai, I.; Nambu, A.; Nakamura, T.; Ohta, T. *Chem. Phys. Lett.* **2005**, *413*, 267.

Conclusions

In summary, we have demonstrated the capability to obtain a 2D distribution of isolated {Cr_7Ni} clusters exploiting the direct binding of sulfur-functionalized derivatives on a gold surface. The submonolayer of **1** presents a higher coverage (15−25%) compared to **2** (5−9%). The stoichiometric behavior of the core level intensities, which are the direct fingerprint of the ring, confirms that the ring integrity is preserved. The stability of the clusters in the STM images and the S-2p binding energies indicate a strong molecular grafting with the Au surface for both the functionalizations. The STM height profiles agree with a preferred "quasi-flat" orientation of the clusters. Both STM and XPS reveal the formation of a first SAM formed by free ligands which break from the core of the cluster. In order to increase the saturation coverage of the molecular nanomagnet's submonolayer distribution, we are developing new {Cr_7Ni} derivatives with sulfur ligands strongly bonded to the core of the cluster, in order to avoid the competitive chemisorption of the clusters and of the SAM formed by the free ligands.

Experimental Section

All reagents were from Aldrich and were used as received.

1. $CrF_3 \cdot 4H_2O$ (2.0 g, 11.0 mmol), thiophene-3-carboxylic acid (10 g, 78.0 mmol), dipropylamine (0.7 g, 9.6 mmol), and $2NiCO_3 \cdot 3Ni(OH)_2 \cdot 4H_2O$ (0.2 g, 0.34 mmol) were heated in a Teflon flask at 150 °C for 1 h with stirring. During this period, a green solid formed. After 1 h, the flask was cooled to 100 °C, and toluene (30 mL) was added with stirring. The solution was then refluxed for 5 h, the toluene was removed by distillation, the solution was allowed to cool, and MeCN (20 mL) was added. The resulting microcrystalline product was washed with a large quantity of acetonitrile and dried in the air. The product was recrystallized from THF/toluene. Yield: 2.72 g (63.6% based on Cr). Elemental analysis calculated (%) for $C_{86}H_{64}Cr_7F_8NNiO_{32}S_{16}$: C 38.10; H 2.38; N 0.52; Cr 13.43; Ni 2.16; S 18.92. Found: C 37.74; H 2.08; N 0.47; Cr 13.64; Ni 2.17; S 18.79. Electrospray-MS (THF) *m*/*z*: +2813 [M + $(C_3H_7)_2NH_2]^+$.

2. Me_3CCOOH (15 g, 147 mmol) and 2-(butylamino)ethanethiol (1.8 g, 13.5 mmol) were heated briefly, with stirring, in a Teflon flask at 140 °C to obtain a homogeneous solution. To that solution was added $CrF_3 \cdot 4H_2O$ (5.0 g, 27.6 mmol), and then the mixture

was heated for 2 h. During this period, the chromium fluoride dissolved to produce a green solution, and to that was added $2NiCO_3{\cdot}3Ni(OH)_2{\cdot}4H_2O$ (0.5 g, 0.85 mmol). The temperature was then increased to 160 °C, and the flask was heated for a further 4 h. After this, the flask was cooled to room temperature, and acetone (30 mL) was then added with stirring. The green crystalline product was filtered and washed with acetone and then dissolved in pentane (60 mL). The pentane solution was filtered, and the filtrate was diluted with acetone (30 mL). Concentration of the solution by evaporation at room temperature produces green crystals of X-ray quality. Yield 6.1 g (66.4% based on Cr). Elemental analysis calculated (%) for $C_{86}H_{160}Cr_7F_8NNiO_{32}S$: Cr 15.64; Ni 2.52; C 44.39; H 6.93; N 0.60; S 1.38. Found: Cr 15.81; Ni 2.51; C 44.78; H 7.16; N 0.56; S 1.35. Electrospray-MS (sample dissolved in THF, the spectra run in MeCN) *m*/*z*: +2349 $[M + Na]^+$; −2192 $[M - HS(CH_2)_2NH_2C_4H_9]^-$.

X-ray Diffraction Studies. Data were collected on a Bruker SMART CCD diffractometer (Mo Kα, $\lambda = 0.710\,69$ Å). In all cases, the selected crystals were mounted on the tip of a glass pin using Paratone-N oil and placed in the cold flow (120 K) produced with an Oxford cryocooling device.[27] Complete hemispheres of data were collected using ω-scans (0.3°, 30 s/frame). Integrated intensities were obtained with SAINT+,[28] and they were corrected for absorption using SADABS.[28] Structure solution and refinement were performed with the SHELX-package.[28] The structures were solved by direct methods and completed by iterative cycles of ΔF syntheses and full-matrix least-squares refinement against F^2. The results for **1** and **2** are summarized in Table 2. Only a limited data range is available from these ring structures.

For **1**, disorder in the ring structure is present not only in the position of the Ni atom but also in the position of Cr2 and Cr3. This disorder cannot be modeled using twin laws and requires a partial split of the whole ring structure. The disorder of the Ni atom has been accounted for by splitting it between all metal sites. The limited data have led to C atoms being modeled isotropically. For **2**, the Ni position could not be identified and has therefore been disordered over all metal sites. The pivalate ligands also show significant disorder which has been modeled with split sites. The central amine is also disordered over two sites. In both structures hydrogen atoms have been placed in calculated positions.

CCDC 615268 and 615269 contain the supplementary crystallographic data for this paper. These data can be obtained free of charge from the Cambridge Crystallographic Data Centre via www.ccdc.cam.ac.uk/data_request/cif.

Table 2. Experimental Data for X-ray Diffraction Studies of **1** and **2**

	1	**2**
formula	$C_{90}H_{70}Cr_7F_8N_3NiO_{32}S_{16}$	$C_{86}H_{159}Cr_7F_8NNiO_{32}S$
M	2793.16	2325.91
crystal system	orthorhombic	monoclinic
space group	*Pnma*	*C*2/*c*
a/Å	26.830(2)	26.018(3)
b/Å	29.051(2)	20.150(2)
c/Å	16.3579(15)	26.169(3)
β/deg	90	111.027(10)
U/Å^3	12749.9(17)	12806(2)
T/K	100(2)	100(2)
Z	4	4
μ/mm^{-1}	1.455	1.206
unique data	6942	11293
data with $F_o > 4\sigma(F_o)$	3380	4322
R1, wR2[a]	0.0914, 0.2802	0.0981, 0.2871

[a] R1 is based on observed data, wR2 is based on all unique data.

Surface Studies. The substrates exploited are both Au(111) single crystals cleaned by repeated cycles of sputtering−annealing and flame-annealed Au films evaporated on mica. The sulfur-functionalized derivatives were deposited from the liquid phase by immersing the gold substrate in freshly prepared millimolar solutions of **1** and **2** in tetrahydrofuran. After that they were thoroughly rinsed with pure THF to remove weakly adsorbed molecules on the surface. Different concentrations (from 1 to 9 mM), deposition times (from 10 s up to 20 h), and solvents (ethanol, THF, dichloromethane) were tested. Because of the higher solubility level, we have used THF as the solvent. STM measurements were carried out with a commercial UHV SPM Omicron apparatus. All STM images were acquired in a constant-current mode with bias voltages of 2.0 V and a very low tunneling current of 30 pA, in order to avoid dragging or damaging such soft organic materials with the STM-tip. The STM tips used are tungsten wires that were cut under ambient conditions and then electrochemically etched. XPS measurements were performed using an Omicron hemispherical analyzer (EA125) with an Mg Kα X-ray source (1253.6 eV).

Acknowledgment. This work was supported by the EU Research and Training Network "QueMolNa", the EU Network of Excellence "MAGMANet" and the EPSRC (U.K.).

IC0624266

(27) Cosier, J.; Glazer, A. M. *J. Appl. Crystallogr.* **1986**, *19*, 105.
(28) *SHELX-PC Package*; Bruker Analytical X-ray Systems: Madison, WI, 1998.